Greenhouse gas intensity of geologic hydrogen produced from subsurface deposits

Adam R. Brandt
Department of Energy Science & Engineering
Stanford University
abrandt@stanford.edu
+1-650-724-8251

Version: March 22nd 2023

Abstract

Geologic hydrogen (H_2) deposits could be a source of climate friendly energy. In this work, we perform a prospective life cycle assessment of a generic geologic hydrogen production and processing system. While it is still too early in the development cycle to estimate precise life-cycle carbon intensities (CI) we can use fundamental engineering physics and chemistry to estimate CI. Our baseline case includes gas with 85 mol% H_2, and remainder N_2 (12%) and CH_4 (1.5%) and other inert gases (1.5%). We set baseline productivity, depth, and other producing parameters using data from US natural gas wells drilled to date. We use a modified version of the OPGEE open-source oil & gas life cycle assessment tool to model the energy use and emissions from geologic hydrogen systems. Producing, dewatering, separating, and (if needed) compressing the gas results in a site-boundary GHG intensity of ~0.4 kg CO_2eq. GHG per kg of H_2 produced for the baseline case, or ~3 gCO_2eq./MJ LHV H_2. The largest sources of GHG emissions are fugitive losses from the system and embodied emissions in constructed wellbores and equipment. Sensitivity analysis is performed by examining varying gas compositions, as wells other resource parameters and production methods. We find that results are most sensitive to the gas composition – mainly the amount of H_2 and CH_4 in the raw gas stream. Other key drivers include how the process is powered and fueled, and the methods of handling and disposing of the separated non-H_2 species.

Introduction

The need for a shift to climate-friendly energy sources has become urgent. A key strategy for this transition will be electrification of end uses coupled to a shift to clean electricity sources (e.g., renewables). However, some end uses, particularly in heavy shipping and industry, may require gaseous fuels for reliability, energy density, and process chemistry reasons. Also, deliverability of energy in the winter may be aided by having a carbon-free chemical energy carrier. Hydrogen has been widely proposed as a fuel that can meet these needs. Hydrogen is currently produced from natural gas via steam-methane reforming (SMR, the current dominant method), or via electrolysis of water using renewable energy. However, another less-explored option exists: geologic hydrogen produced from subsurface hydrogen accumulations (also called "natural hydrogen"). Geologic hydrogen has been shown to exist in geologic deposits around the world, and has been discovered in the course of exploring for natural gas[1-3] as well as in exploratory geologic drilling.[4,5] Deposits have been found across the Earth: in the United States[6], Canada and Finland[7], the Phillipines[8], Australia[9], Brazil[10], Oman[11] and Turkey,[12] and Mali[13], as well as near seafloor geologic activity such as hydrothermal vents and mid-ocean ridges.[4,5] See Zgonnik[1] for a comprehensive review of this literature.

Geologic hydrogen has not been commercially developed at scale to date, and wells have only recently been drilled for purposeful production. The first hydrogen well was discovered accidentally in Mali, where explosive gas was encountered while drilling for water in 1987.[13] The well was re-opened in 2011 to production, and since then a series of 18 exploratory wells have been drilled to delineate the deposit. These wells are of various depths and have found H_2 in a stack of 5 reservoirs between 100 m and 1800 m deep (300-6000 ft).[13] In 2019 an initial well was drilled in Nebraska USA by Natural Hydrogen Energy in 2019 to a depth of 3400 m (11,200 ft).[3] Fewer data are available on the Nebraska well with no gas composition or well productivity data reported.

For geologic H_2 to form a useful part of future clean energy systems, two key questions exist. First: will geologic H_2 be available in commercial quantities? And, second: will geologic H_2 be able to be produced and processed in a way that leads to low overall life cycle carbon intensity (CI)?

The first key question hinges mostly on the scale of the geologic hydrogen resource. To date, drilling has not been focused on areas prospective for H_2, and therefore availability remains an open question. Zgonnik[1] and others[3,9] argue that the methods commonly used to assess gas composition are insensitive to H_2, as H_2 is often used as the carrier gas in analytical equipment (i.e., gas chromatography). This potentially leads to systematic under-estimation of the prevalence of H_2 in the sub-surface. The mechanisms by which geologic H_2 is formed are also debated, with some proposed paths being: (1) radiolytic byproduct of natural nuclear decay; (2) rock weathering reactions which consume oxygen from subsurface waters leaving an excess of H_2; (3) microbial degradation of hydrocarbons or other forms of organic matter; or (4) seepage of primordial H_2 from deep in the earth.

The second key question -- "what is the life cycle carbon intensity (CI) of geologic hydrogen?" -- is also important. But no work to date has examined the prospective CI of geologic H_2, given its

relative novelty and lack of commercial production experience. In this paper we aim to estimate the range of likely CI values that might result from geologic H_2 production. This is meant to be a *first assessment* of a generic geologic H_2 production process, not a specific assessment of any given commercial deposit. This analysis is performed in the spirit of "prospective LCA for emerging technologies" as discussed in Bergerson et al.[14] The purpose of a prospective LCA is not to definitively examine the environmental impacts of a technology, but to use early information about a fundamentally new technology to make a first assessment of environmental impacts or benefits, in order to guide further investment and development. The concept is that early stage LCA can help diagnose environmental concerns early in technology development or readiness to avoid sunk costs of investment into technologies that are unlikely to be environmentally beneficial.

In this paper we explore the prospective CI of geologic H_2 using a modified version of an open-source oil and gas GHG calculation tool, the OPGEE model (Oil Production Greenhouse Gas Emissions Estimator). OPGEE was first developed by El Houjeiri and Brandt[15], and collaborators and has been used in numerous papers[16-21]. OPGEE uses petroleum engineering fundamentals and the properties of a given oil and gas resource to estimate possible GHG emissions. OPGEE is documented in 400+ pages of documentation[22]. OPGEE v3.0a is our basis model which is modified to represent geologic H_2 production. The modified model is available as supporting information (SI) attached.

Because the OPGEE model estimates emissions based on conventional oil and gas production, some modifications and extensions to the model are made to represent geologic hydrogen production. Key changes include modification of gas processing equipment calculations to account for differing composition of the gas, as well as addition of a simplified pressure-swing absorption (PSA) unit for gas purification.

We examine numerous cases, with a focus on cases employing designs to reduce CI, excluding cases that would likely have high climate impact and therefore are unlikely to be implemented in a clean energy future (e.g., a case where entrained methane is separated then vented). We explore variations in the geologic and chemical properties of the resource, variations in the treatment and disposition of the waste gas stream produced during gas purification, as well as variations in the source of energy for the gas processing and compression equipment. We compute GHG intensity for these cases in terms of life cycle CI measured in $gCO_2eq.$ GHGs per MJ LHV of H_2 produced, as well as kg $CO_2eq.$ GHGs per kg of H_2 produced. The functional unit is 1 kg of H_2 produced at above 99% purity and above 3 MPa (435 psi) pressure, aligned with US DOE documentation.[23]

More details about modeling and case definitions are provided below in the methods section. After these methods are outlined, results are presented and the implications and limitations are discussed. The associated baseline case OPGEE model is included as supporting information (SI).

Methods

The baseline process flow diagram used in our assessment is shown in Figure 1. The OPGEE 3.0a model is used as the basis for this modeling effort, available for free download and unrestricted use. Changes were made to the OPGEE model in the following broad areas that are described in more detail below: (1) gas composition and gas properties; (2) added hydrogen-specific aspects of gas processing and gas compression; (3) added gas separation via PSA; (4) added ability to consume product hydrogen for process needs. After these changes are described, we outline the cases and their definitions, and describe the data inputs used.

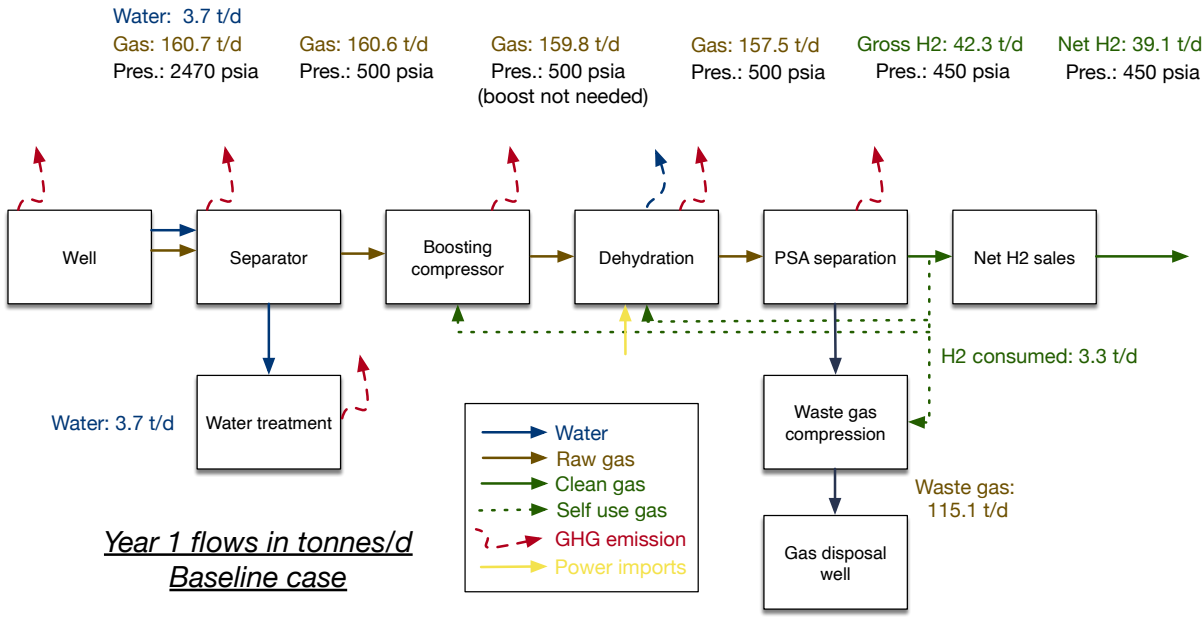

Figure 1. Process flow diagram for the baseline case. Flow rates in tonnes per day are evaluated in Baseline case, year 1. Boosting compressor is not needed because separator can be easily choked to 500 psi inlet requirement for dehydration.

As SI, the baseline model as modified OPGEE v3.0a is attached to this paper. In the baseline model, changes from OPGEE 3.0a are highlighted in orange cells, which appear on tabs with their color changed to orange. This is to allow for understanding by readers differences between OPGEE 3.0a and the modified version used here.

Gas composition and gas properties

We collect data on gas composition from the literature. H_2 exists naturally in mixtures of multiple gases. Zgonnik[1] includes an extensive literature review, incorporating data from decades of geologic literature, while Vacquand[12] and Prinzhofer[13] present ternary diagrams showing broad "regions" of composition. Zgonnik includes extensive tables of 100s of gas samples wherein gas composition of greater than 10% H_2 was observed. Some comments about the composition data:

- Samples with greater than 90 mol% H_2 have been observed in countries such as Belarus, Cyprus, Gabon, Germany, Japan, Kazakhstan, Mali, Oman, Russian Federation, USA, and Uzbekistan.
- Samples with greater than 90 mol% H_2 have been observed in types of samples including Ophiolites, rift zones, Precambrian rocks, in volcanic gases, in orebodies, in coal basins, in sedimentary basins, and in salt deposits.
- Samples with greater than 80 mol% H_2 are seen in even more locations and types of deposits.

A mix of non-H_2 gases is also generally present as the remainder of the gas in a deposit. Chief among these non-H_2 species are N_2 and CH_4, with non-trivial fractions of He in some cases, as well as Ar and other noble gases. Due to the reducing environment present in these deposits, CO_2 is generally not prevalent. Ternary diagrams[12,13] show clusters of composition suggesting "types" of formations. Regions such as Mali, Kansas, and Oman have some samples with nearly all N_2 as non-H_2 fraction, (along with small amounts of other inerts like Ar and He). In contrast, samples from Turkey and Philippines, instead contain mainly CH_4 as the non-H_2 species, likely indicating a different formation mechanism wherein abiogenic CH_4 might be formed by thermogenic reaction of H_2 with C-containing species like dissolved CO_2.[12] Mixed cases exist, such as New Caledonia[12], which displays both N_2 and CH_4. In those mixed samples, N_2 is typically seen with 3x-10x larger mole fraction than CH_4. We use these data to derive baseline and alternative gas composition cases (see below).

By default, H_2 is tracked in the OPGEE flowsheet system as one of the possible components of each gas phase stream. However, the basic OPGEE inputs sheet does not have the feature to specify an H_2 mole fraction due to the uncommon occurrence of H_2 in typical gas reservoirs. Therefore, we instead insert the modified H_2-containing gas composition directly into the sheet "Separation", where it would normally enter the processing stream.

We add thermodynamic and physical properties of H_2 that are needed for modeling but not included in OPGEE 3.0a. First, we add non-ideal gas compressibility factors (Z-factors) for H_2 as a function of pressure and temperature from the same source used to generate tabulated Z-factors for other species treated in this way in OPGEE 3.0a, the NIST REFPROP chemical and thermodynamic properties database[24]. Data tables are returned for a variety of temperatures and pressures and as needed the (rounded) value from the model is looked up from the table by various compressors and other processing sheets. Regarding solubility of gas in water, data for the Henry's law constant for H_2 are taken from NIST.[25] Data are obtained for Henry's law constants at standard temperature (273.15 K) as well as for the temperature dependence of the constant $dK_H/d(1/T)$.

Second, we require a global warming potential (GWP) of hydrogen that is lost as fugitive emissions or leakage to the environment. H_2 has no direct warming effect on the atmosphere, but instead has a secondary GWP due to the fact that H_2 reacts with atmospheric hydroxyl radicals (OH^-).[26] These OH^- radicals are the main destruction pathway for CH_4, as well as other atmospheric pollutants. Thus, reactions with H_2 can consume OH^- and potentially result in longer lifetimes for CH_4. The baseline estimated resulting GWP used is from Derwent et al. 2020[27], who estimate a GWP_{100} of 5+/- 1. This is similar to the GWP from Derwent et al. 2006[28], of 5.8 and

other work by the same authors[29]. Another key group examining the GWP of H_2 is that of Warwick.[30,31] For a higher estimate, we use the estimated GWP_{100} from Warwick et al.[30], who estimate a GWP_{100} of 10.9, significantly higher than that of Derwent and other reports. This is due to the fact that Warwick et al.[30] include stratospheric effects as well as tropospheric effects. Because consensus on H_2 GWP has not emerged in the literature, we include both cases here.

Lastly, the equilibrium water vapor (moisture) content of a stream of gas depends on its composition. In OPGEE 3.0a, oil and gas industry correlations are used to estimate the amount of moisture in the natural gas streams.[22] For geologic H_2, we are dealing with mixtures of predominantly H_2 and N_2, both of which are poorly represented in hydrocarbon industry correlations. Moisture present in H_2 is given by water loading chart of Huang[32], which presents absolute humidity of H_2 as a function of temperature and pressure. Moisture present in N_2 is given by Luks et al.[33], who tabulated moisture present in N_2 at various experimental conditions. We use Luks et al.[33] supplementary table S7 for pure N_2, averaging the quantities for 10 and 50 atm pressure to approximate separator conditions.

Well completion

Wells are assumed to be drilled into conventional reservoirs and are assumed to not require horizontal drilling or hydraulic stimulation. Well completion fugitive emissions are modified from OPGEE v3.0a default values[22] because OPGEE default values assume a typical natural gas composition for the emitted gases for gases released during well drilling and completion. In our case, we assume that the total mass of gas released during the completion event is the same as a conventional well as per OPGEE v3.0a defaults, but that the gas which is emitted is of the composition of the case being modeled (e.g., 85vol.% H_2 in the baseline case). This results in lower GHG emissions from drilling and completion due to the predominance of H_2 and N_2 in the drilling fugitives rather than primarily CH_4 as would occur in a conventional natural gas well.

Equipment use and fugitive emissions

Geologic H_2 production will require somewhat different producing equipment compared to conventional natural gas. First, we turn off process units that are typically used in OPGEE v3.0a for modeling natural gas production but are not needed for geologic H_2 production. We turn off the acid gas removal (AGR) unit, as studied gas compositions do not include CO_2 and H_2S. Second, we turn off the demethanizer/fractionation unit as there are not higher hydrocarbons (C_3+) in appreciable quantities to be removed from the stream.

Next, the liquids handling infrastructure is changed. The liquid hydrocarbon tank is removed, as geologic H_2 deposits are not thought to be associated with condensable hydrocarbons. This removes a point of methane leakage common in oil producing operations. Second, the water handling infrastructure modelling is improved to include degassing and emission of gas CH_4 and H_2 dissolved in water using above Henry's law constants.

Hydrogen-specific aspects of gas processing and gas compression

Hydrogen-specific aspects of gas processing are included in the model for gas separation, gas compression, and gas dehydration.

For gas separation, we account for dissolved H_2 in the water stream leaving the separator using the Henry's law relationships described above. We account for water content leaving the separator at high pressure and temperature, as well as water leaving the atmospheric storage tank at ambient conditions. The difference between these quantities represents the gas that would be flashed upon water entering the atmospheric pressure storage tank. This flashed gas stream then enters the tank gas handling system where it is either recompressed and recovered, flared, or vented, depending on OPGEE settings (baseline case is that these emissions are not captured and are added to onsite tank vents). Because neither CH_4 nor H_2 are highly soluble in water, these quantities are small.

For gas compression, we account for the differences between compressing H_2 and compressing hydrocarbon gases. Required thermodynamic properties such as critical point properties and specific heats ratio are already included for all species in OPGEE v3.0a for standard conditions, including for H_2. However, OPGEE v3.0a uses gas compressibility factor correlations developed for the oil and gas industry. These correlations are commonly used in the natural gas industry, but they are well suited for mixtures of hydrocarbon gases, or with corrections, hydrocarbons containing acid species like CO_2 and H_2S. They are not designed for mixtures of (mostly) H_2 and N_2. In our modified model, the non-ideal behavior of H_2 and N_2 is calculated by adding a supplemental table to look up the compressibility factors (Z-factor) for H_2 and N_2 from tabulated NIST data described above. These factors are then used in the compressor work calculations. This extends the approach already implemented in OPGEE v3.0a for non-hydrocarbon gases. To check the modeling accuracy, we constructed a case aligned with the Argonne National Laboratory HDSAM (Hydrogen Delivery and System Analysis Model) v3.1 compressor calculations.[34] We find agreement (<10% deviation) in overall compressor sizing and work requirements compared to the basic compressor outlined in Argonne's model (see SI).

The OPGEE gas dehydration unit is included and turned on, as water vapor should be prevented from entering the PSA unit. The calculated moisture content of our baseline separated gas mixture at the gas dehydration unit inlet is 0.014 tonnes H_2O/tonne gas, or slightly in excess of 1% by mass water vapor. For gas dehydration, we model dehydration of the gas stream by default using the same glycol (TEG) dehydration unit as in OPGEE v3.0a. As a supplement, we compare this to a silica gel dehydration process, which is more similar to that used in electrolytic hydrogen production. A standard silica gel process design model is used from Coker et al.[35] including the heat of desorption of water from silica gel, sensible heat for media and reactor body, and heat loss factors. The amount of energy estimated for silica gel dehydration was within 5% of that estimated using TEG dehydration unit, so the choice of dehydration technology will not have a large impact on process CI.

Gas separation via PSA

Next, we augment OPGEE v3.0a by adding a simple pressure-swing adsorption (PSA) unit. A PSA operates by selectively adsorbing species to a contacted media at high pressure, then "blowing down" the reactor to low pressure to reject the adsorbed species. H_2 is more weakly absorbed than other gas species, so PSA is commonly used to purify H_2. For example, refinery H_2 production processes commonly use PSA to separate H_2 from CO_2 in the output streams of a SMR reactor. In our model, high pressure impure gas is introduced into the reactor at 500 psia, within the ranges for existing PSA systems[36,37]. Nearly pure H_2 emerges at slightly lower pressure as the reactor selectively adsorbs other gases (in our case N_2 and CH_4).

After the reactor is fully loaded, flow is shut off, and the reactor containing the waste gases is depressurized into a waste gas process line, blowing down the adsorbed waste gas. Pressure drop on the product stream is 50 psi (500 to 450 psia), while the waste gas stream is blown down from 500 to 25 psia to ensure complete desorption of waste gas. We assume complete separation of waste gas products from H_2, (e.g., H_2 mol% of product gas >99%) but also account for inefficiency of separation by assuming 10% of incoming H_2 is lost into the waste gas stream as "slip". This slip of H_2 into the waste gas stream is reported in the literature as ranging from 5-20%,[36,37] but little literature covers mixtures of H_2/CH_4/N_2, as this is not the common application of PSA (PSA is heavily used in steam-methane-reforming systems, which have a different composition).

Some literature-reported geologic H_2 samples contain He in addition to H_2. Because of the similarity of these gases, slip of He into the PSA H_2 product stream is likely. The economic value of He makes it possible that this could be another revenue stream for producers, but assessment of H_2/He separation options is beyond the scope of this work. We include He with Ar as "other inerts" in this study, and assume for simplicity that a separation process can be designed. Future studies should use detailed chemical process models to examine slippage of both H_2 into the waste gas stream and He into the product gas stream.

Consumption of H_2 for process needs

The Baseline case assumes that process combustion energy and heat requirements are self-fueled using clean product H_2. This would result in the lowest CI due to the lack of combustion of carbon-containing gases. In some cases, electrical energy inputs are required by the OPGEE model structure and are unlikely to be replaced with hydrogen. For example, pumps for dehydration solvent circulation and water treatment pumping. However, the larger uses of dehydration solvent thermal regeneration and compressor power are assumed to be powered via hydrogen combustion.

In alternative cases outlined below in Table 3, we also examine cases where the processes are fueled with waste gas from the PSA, by imported natural gas, by imported green electricity, or by imported US-average electricity. See case definitions below.

Cases and definitions

Important assumptions for the baseline case are outlined below in Table 1. Table 2 then gives details for the alternative gas compositions cases. Table 3 gives details for other alternative cases. The baseline case is meant to represent a "general" case with average properties.

While commercial development would be favored by higher H_2 concentration, and we would expect commercial producers to focus on such sites, it is still too early to known whether it is realistic to expect large number of sites with very high H_2 concentrations to be found. For this reason, we choose a baseline case with a high concentration (85 mol%) as might be selected by a developer, but conservatively assume that reservoirs near the highest concentrations seen in the literature of 95+ mol% H_2 may be too challenging to find to exploit at scale. Our baseline case is selected to be of the N_2-rich type of reservoir. This type was chosen because the existing commercially drilled wells in Mali and central US (Kansas/Nebraska) tap these types of deposits, and they are likely to have the largest potential for low-CI energy. We perform sensitivity analysis on gas composition below, examining two alternative cases with more CH_4 (a mixed case and a CH_4-rich case).

In our baseline case we assume 15% non-H_2 gas is primarily N_2 (12%) with smaller amounts CH_4 (1.5%) and Ar/He other (1.5%). This is similar to Mali and Kansas sample clusters in the literature[12]. It is also near the lower CH_4 limit of the "N_2-H_2-CH_4 type" mixed class defined by Vacquand et al., where the lowest CH_4 contribution is ~10:1 N_2:CH_4 molar ratio. We also explore cases where the remainder of the gas is mixed (66% N_2, 33% CH_4) or almost exclusively CH_4 (as in Phillipines or Turkey). These alternative cases allow us to explore the effects on CI of the GWP of the remainder gas. These are called "mixed CH_4/N_2" and "High CH_4" cases, respectively.

In addition to varying the minor species, we also explore overall H_2 concentration. Alternative cases with lower (75%) and higher (95%) H_2 concentrations are chosen as sensitivity cases. These are termed the "Low H_2" and "High H_2" cases respectively. We also explore two sub-types of the Low H_2 case as well, wherein the remainder gas (25 mol%) is made up either mostly CH_4 ("Low H_2 w/ CH_4") or N_2 ("Low H_2 w/ N_2"). Lastly, we sweep across a wide range of H_2 concentrations from 50 mol% to 100 mol% with varying residual gas composition across pure N_2 or CH_4 end members.

Another key baseline case factor is the volumetric productivity of wells. Detailed discussion of the sources for productivity data is given in SI below. Briefly, the baseline case uses production rates, well depths and other factors typical of North America gas wells (based on ~1 million gas wells drilled since 1920 available from a commercial database). We also run a low productivity case that is more pessimistic about the productivity of H_2 wells in case they are less prolific than traditional gas wells.

Table 1. Baseline H_2 field parameters for analysis. Definitions: BCF = billion cubic feet, mmscf = million standard cubic feet, psia = pounds per square inch, absolute, bbl = barrel.

Parameter	Baseline value	Unit	SI Value	SI unit
Total producing wells	50	wells	50	wells
Raw Gas EUR	67	BCF	1.89	Bm^3
H_2 EUR	57	BCF	1.61	Bm^3
Depth	6,000	ft	1829	m
Initial reservoir pressure	2520	psia	17.78	Mpa
Initial flow rate	23.1	mmscf/d	0.65	Mm^3/d
Well lifetime	30	years	30	years
Pressure drop	5%	% per year	5	% per year
Production decline rate	var.	% per year	var.	% per year
Gas Composition				
H_2	85.0	mol %	85.0	mol %
N_2	12.0	mol %	12.0	mol %
CH_4	1.5	mol %	1.5	mol %
C_{2+}	0.0	mol %	0.0	mol %
Ar + He + oth.	1.5	mol %	1.5	mol %
Num. of boost comp.	2	comp.	2	comp.
Num. of purification plants	1	plant	1	plant
Water cut	1	bbl/mmscf	5.6	L/Mm^3
H_2 purification loss rate	10	% loss	10	% loss
BCF per well	1.33	BCF	37.66	M m^3

Table 2. Mole percents of produced raw gas for variations in gas composition cases. All compositions exclude equilibrium water vapor.

Case	Mole percent [mol%]				
	H_2	N_2	CH_4	Ar/He/oth.	Tot.
Baseline	85	12	1.5	1.5	100
High CH_4	85	1.5	12	1.5	100
Mixed CH_4/N_2	85	8.5	5	1.5	100
Low H_2	75	20	2.5	2.5	100
High H_2	95	4	0.5	0.5	100
Low H_2 w/ CH_4	75	2.5	22.5	0.0	100
Low H_2 w/ N_2	75	22.5	2.5	0.0	100

Table 3. Other sensitivity cases, changing parameters other than gas composition

Case	Parameter	Baseline value	Sensitivity value	Unit
Low pressure	Reservoir pressure	2520	630	psia
High pressure	Reservoir pressure	2520	5040	psia
Low productivity	Per-well EUR	1.33	0.33	BCF/well
High productivity	Per-well EUR	1.33	2	BCF/well
High H_2 GWP	H_2 GWP_{100}	5.0	10.9	kg CO_2 eq./kg H_2
Flare waste gas	Waste gas fate	Reinject	Flare	-
Use waste gas then reinject	Consume waste gas	Reinject	Use waste gas for process energy	-
Imported NG	Gas imports	None	Import gas	-
Electric power – Renewable	Electric imports	None	Import renewable power	-
Electric power – US Average	Electric imports	None	Import US average power	-
Embodied emissions	Embodied emissions	On	Off	-
Small sources	Small sources adder	10% of directly estimated	0.5	$gCO_2eq./MJ$

In most sensitivity cases the changes are straightforward alteration of a single parameter (e.g., H_2 GWP) or a vector of parameters (e.g., gas composition vector). In the "Imported NG" sensitivity case, we negate the self-consumption of produced hydrogen, replacing it with OPGEE default imports of natural gas. In the "Electric Power – Renewable" and "Electric Power – US Average" cases we shift loads for compression and solvent regeneration to electricity and set the electric power fuel mix and CI to the appropriate settings. In the renewable case, life cycle CI is assumed to be 50% wind and 50% solar life cycle CI, as given by NREL LCA meta-analyses[38,39].

In the case of "Use waste gas then reinject" we re-engineer some aspects of OPGEE flow modeling. First, we change the emissions factor for natural gas combustion, changing the CO_2 portion of the GREET-based OPGEE default emissions factor for natural gas use to one that accounts for the mix of H_2 and CH_4 (on LHV basis) that is present in the waste gas. Because of the H_2 content, the CO_2 intensity of the waste gas per unit of energy is significantly lower than that of natural gas, except in high CH_4 cases. Also, offsite emissions from natural gas imports are voided, as the gas used is on-site waste gas (this happens automatically in self consumption of the final product as in the Baseline case and all other cases with self-use of final product H_2). Lastly, we implement iterative calculation of the amount of gas required to be injected. An iterative solution is required because the amount of waste gas to be injected affects energy use in the waste gas reinjection compressor, which affects the amount of waste gas to be injected, and so on. In the resulting solution, approximately 30-35% of the waste gas is used to power the process, and the rest is reinjected (varies by simulation year).

Results

Baseline case results are shown in Figure 1 and Figure 2. Figure 1 flow schematic for the baseline case shows flows in simulated year 1 of the production process. Self-use of produced clean H_2 is approximately 8% of gross H_2 production, while H_2 lost into the waste gas stream is 10% of gross production. Figure 2 shows the production-weighted mean emissions for the baseline case in bar form on left. Production-weighted mean baseline production intensity is 0.37 kg CO_2 eq. GHGs per kg of H_2 produced over the life of the well. The min-max range in CI is given by the year 1 emissions (min) and year 30 emissions (max), as shown in time trend on right. We do not include other forms of uncertainty in our ranges, because the nascent nature of the industry precludes assigning realistic empirical distributions to the underlying parameters. Emissions increase over time due to reduced well productivity resulting in more fugitive emissions per unit of gas produced and due to apportioning embodied emissions across fewer units of gas produced. The effect of productivity on fugitive emissions intensity has been seen in multiple empirical methane leakage studies and is well-supported by reasonable models of fugitive emissions causation.[40,41] Median CI is slightly above the production-weighted mean.

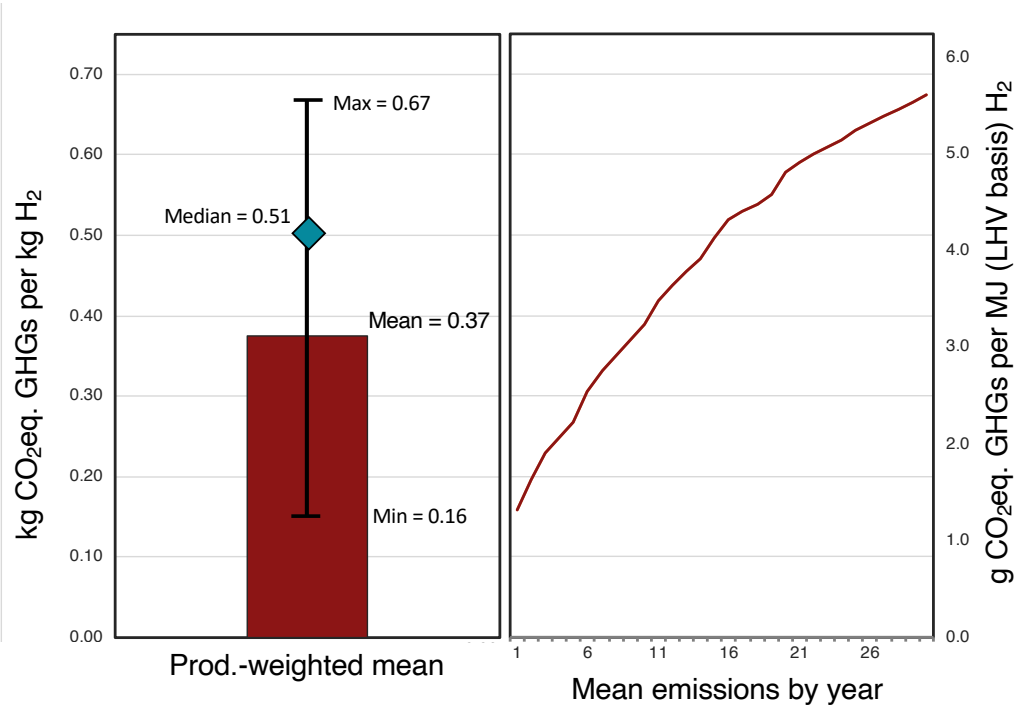

Figure 2: Production-weighted mean emissions for our Baseline case, showing ranges (left) and trend over time (right). Production-weighted mean is more representative than median, and is recommended as the best single indicator, though that is shown for completeness.

Figure 3 shows a detailed breakdown of emissions sources for year 1 in the Baseline case. The emissions are first partitioned into broad stages, such as drilling, production, separation and boost compression, gas processing, and reinjection. Next, within each of these broad stages, we include combustion, venting/flaring/fugitive (VFF) emissions, offsite emissions, and embodied emissions. For clarity, VFF emissions include all purposeful (vented) and un-purposeful (fugitive) emissions from process units and piping. Offsite emissions are emissions that occur

offsite in producing goods, services, energy or other inputs imported to the site. In the baseline case, this category is mostly due to electricity purchases to run remaining electric loads (e.g., dehydration unit solvent circulation pumps), as well as diesel requirements during initial well drilling. In sensitivity cases where the system is electrically-driven or uses imported natural gas, then these offsite emissions are larger. Lastly, embodied emissions refer to emissions associated with steel and cement production for those materials consumed during the construction process. These are mostly due to the drilling stage. Wells contribute the majority of embodied emissions because they require large amounts of steel for multiple layers of casing, as well as cement.

Not shown in Figure 3 are the miscellaneous emissions that OPGEE calls "small sources". In OPGEE is recognized that not all sources will be tracked in any given model. For example, OPGEE does not track energy use in small trucks driven by workers to and from the job site. This term was added to recognize that there are diminishing returns evident in modeling sources, and that there are likely a number of small sources that exist in reality but are not captured by the OPGEE model. In the default case, we set this to be 10% of estimated direct sources, excluding embodied and offsite emissions. We explore a sensitivity case similar to that used in prior OPGEE models where a fixed value of 0.5 $gCO_2eq./MJ$ is used.

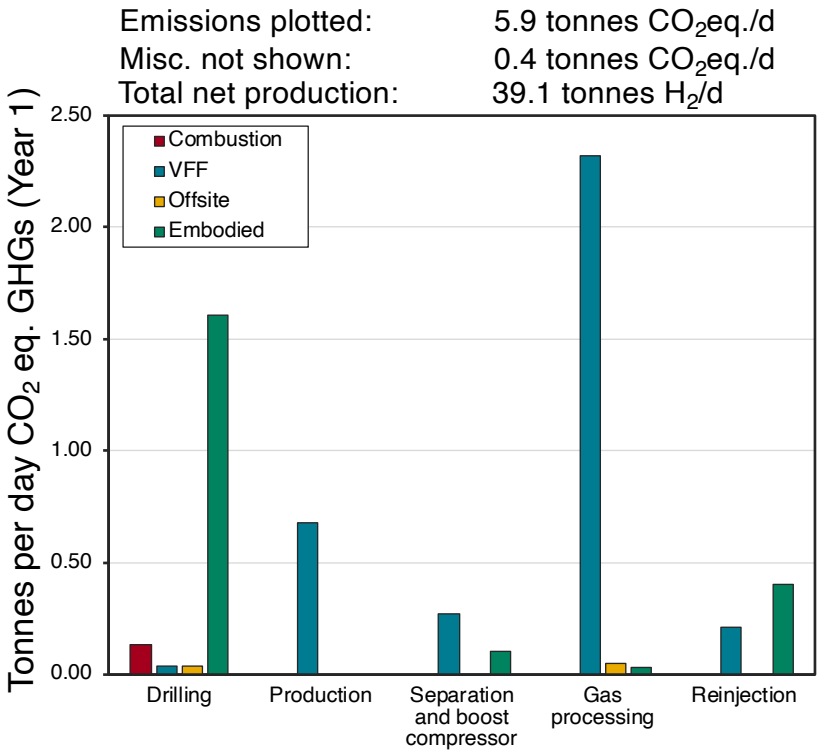

Figure 3: Breakdown of Baseline year 1 emissions sources by type (combustion, offsite, etc.) and by process stage. Miscellaneous "small sources" emissions not plotted because of lack of knowledge about stage and type.

Figure 4 shows the results of sensitivity analysis for all studied sensitivity cases defined above. At the bottom are the results for the baseline case. As in Figure 2 above, the low and high error bars represent year 1 and year 30 emissions intensities as a proxy for variability in emissions from the same project over time.

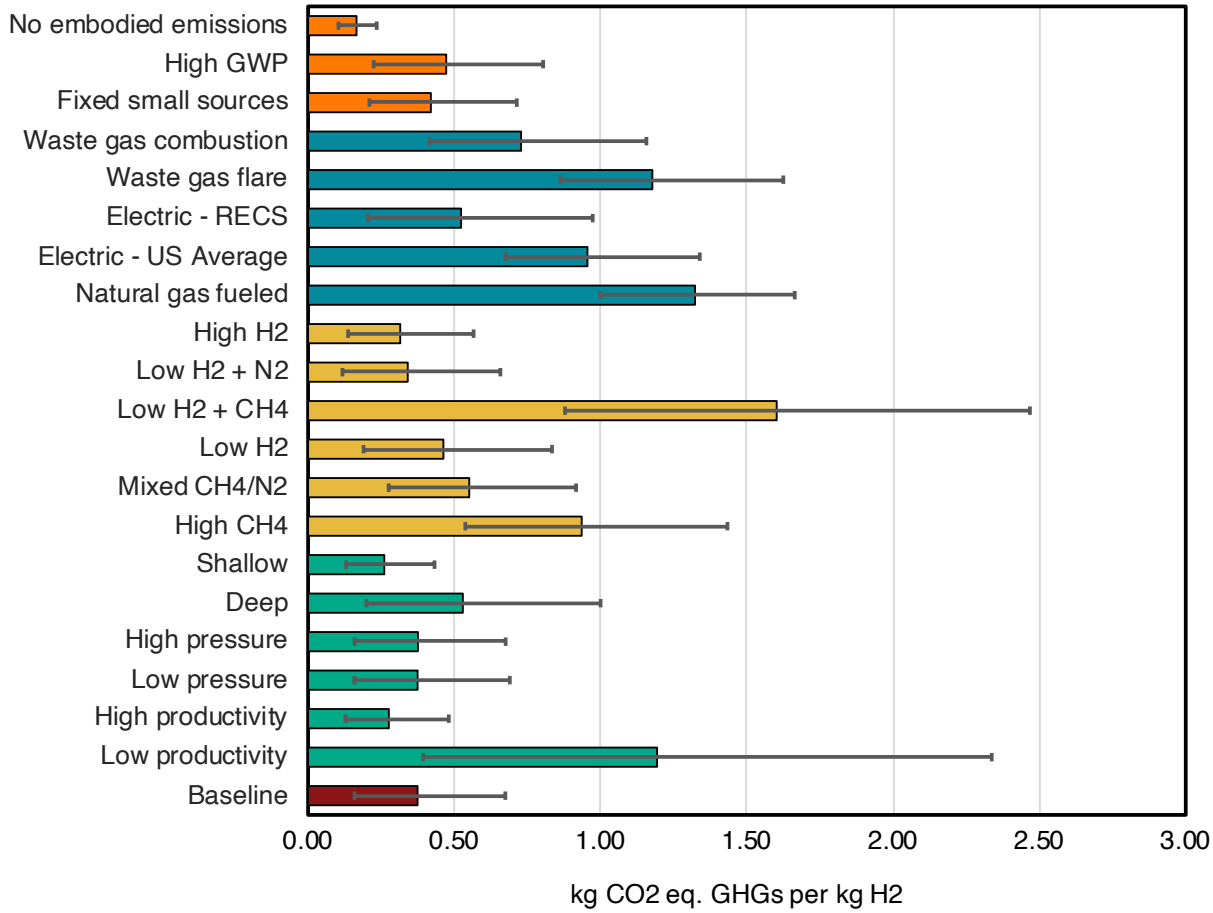

Figure 4: Sensitivity case GHG intensity. See Tables above for definitions of sensitivity cases.

We can see that numerous sensitivity cases have little impact on the carbon intensity.
In contrast, some sensitivity cases do end up causing large changes in CI. First, the disposition of the waste gas matters greatly. While reinjection of waste gas is used in all other cases, dark blue-green bars show cases where (1) the waste gas is used on-site to power systems, then the remainder is reinjected, and (2) a case where waste gas is flared. In the waste gas re-use case about 30% of the produced waste gas is consumed to power the process, and 70% is reinjected. Because of the carbon content of the waste gas (due to CH_4), this results in higher emissions than the baseline case, though note that net H_2 output as product does increase due avoiding self-use of the pure H_2 stream, thus reducing the gross-to-net loss of H_2.

Also problematic is flaring of waste gas. This results in large emissions due to both oxidation of the methane to CO_2 and due to flare slip (OPGEE default values for flare destruction efficiency are used). Importantly, because the waste gas is simply flared, the equipment must still be powered, and therefore net H_2 output to sales is still reduced by the energy requirements of the process. This therefore gives a secondary impact beyond the waste gas consumption case (e.g., the flaring case burns 100% of waste gas rather than 30%, and still consumes ~7% of the produced H_2 to power the process). Thus, flaring the associated waste gas is emissions intensive

compared to other options. This impact of flaring is even larger in cases where the gas composition is rich in CH_4 rather than N_2 or where the H_2 concentration is low.

Next are cases where the operations are powered with carbon containing energy sources. A few effects result. First, these cases avoid the parasitic self-use of ~7-8% of gross H_2 production, resulting in higher net output. However, they result in higher emissions in both the "Electric – US Average" and "Natural gas" cases. In fact, in the natural gas case, it is clearly strictly better to burn the produced waste gas: this is due to avoiding the upstream emissions associated with imported natural gas, and due to the fact that the 10% H_2 slip from the PSA into the waste gas stream means that per unit heating value, the waste gas from our modeled process has lower CI than US average natural gas from OPGEE.

Next are two cases with gas composition high in CH_4 ("High CH_4" and "Low H_2 + CH_4"). This increase in CH_4 results in a number of impacts of note. First, all fugitive emissions along the production and processing chain are made more GHG intensive due to a higher volume fraction of CH_4 in the fugitive emissions stream. Second, the output of useful clean H_2 from the PSA is smaller due to the larger amount of CH_4 in the raw gas stream, rendering all upstream drilling and compression and dehydration emissions larger per unit of useful clean H_2 produced. Third, the amount of waste gas to reinject gets larger, necessitating increased parasitic self-use of produced H_2 and further reducing net H_2 outputs to the consumer. In cases below 75 mol% H_2, this effect gets increasingly large as the concentration drops, due to these interacting impacts (see Figure 5 below).

A major driver is the quality of the resource. In Figure 5 we present the results of "sweeping" across a variety of H_2 mol% values from 50% to 100% H_2, with the remainder gas set to some limiting simple cases [100% CH_4 (red/top), 66% N_2/33% CH_4 (yellow/middle), or 100% N_2 (green/bottom)]. We see that the variation in Figure 5 is larger than that observed in the sensitivity cases presented in Figure 4. Thus, it matters greatly whether reservoirs with high mol% H_2 are available, and absent that, whether reservoirs are available with primarily N_2 as the non-H_2 species. A reservoir with low H_2 concentration is not necessarily emissions intensive, as long as the actual composition is similar to that of our 100% N_2 case.

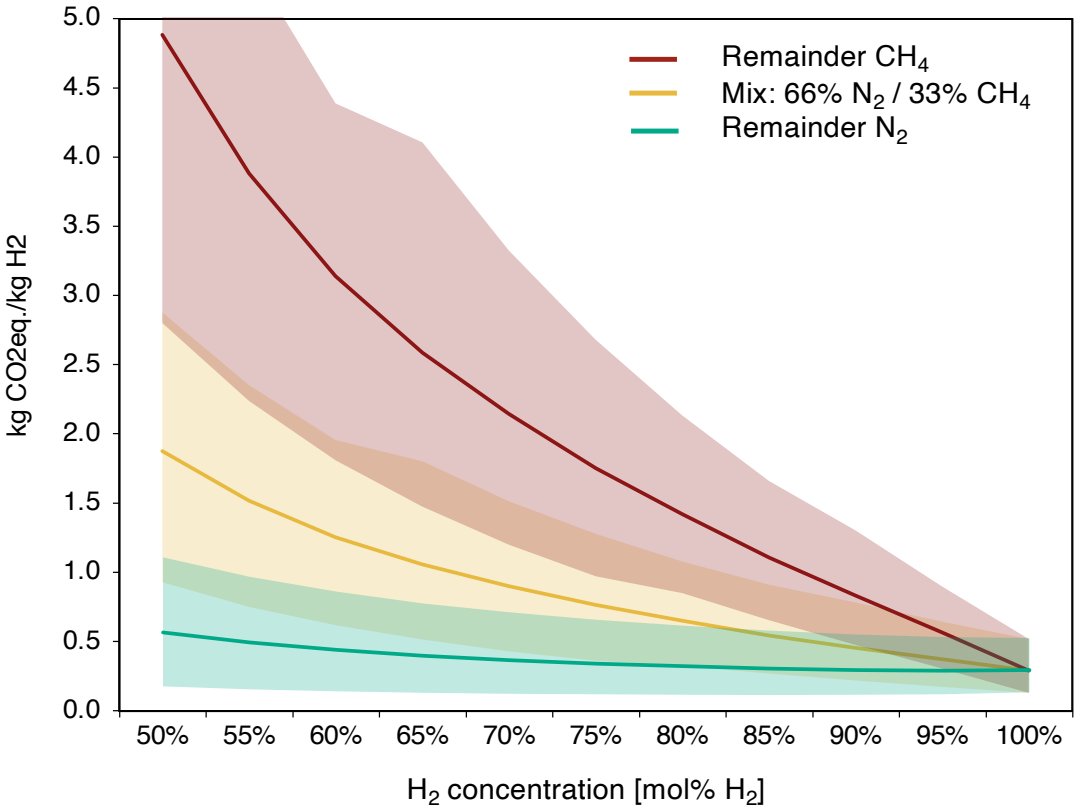

Figure 5. Variation in GHG intensity as a function of H_2 concentration, with remainder gas being either pure CH_4 (red) 66% N_2/33% CH_4 (yellow) or pure N_2 (green).

The last major driver of emissions is treatment of embodied emissions. The importance of these is illustrated by the low emissions in the "no embodied emissions" case, which has a CI well below that of our baseline case. These impacts are also illustrated by the higher emissions intensity of the low productivity case, wherein cumulative production per well drops to 25% of the baseline value (0.33 BCF/well as compared to 1.33 BCF/well), and therefore embodied steel and cement emissions must be apportioned over a smaller amount of energy produced. In some life cycle models, such as the GREET model from Argonne National Laboratory, embodied emissions from various H_2 production processes are not included by default,[42] which would result in figures systematically lower than those produced by OPGEE.

Discussion

This prospective analysis of a "generic" geologic H_2 production process suggests that it is possible to extract low-CI H_2 under reasonable assumptions about gas compositions, pressures, and production practices. If a clean energy source is used to power production processes (e.g., self-produced H_2 or clean power), most of the remaining emissions are due to fugitive emissions of the raw gas during production and processing and embodied emissions. In our baseline case, loss of H_2 as fugitive emissions to the transport inlet is modeled to be 0.8% of total wellhead H_2 production (year 1 value). While in line with other values in the literature (e.g., GREET model assumes 0.62%), diligent operators could possibly outperform this value. In addition to the significant uncertainty regarding fugitive emissions from oil and gas systems in general, it is still

unclear how closely the fugitive emissions rates in OPGEE -- derived from field studies of oil and gas production – will estimate those emissions for H_2 production and processing.

It is worthwhile to compare our results to others from the literature for other sources of H_2, such as renewable-powered electrolysis or SMR with CO_2 capture. We must be careful to select studies with reasonably similar system boundaries. As noted above, the GREET model does not include embodied energy in emissions, so gives wind- and solar-derived H_2 a CI of 0 kg CO_2/kg H_2.[42] Those results are not comparable to our figures here, which do include embodied emissions. Numerous other studies of green and blue H_2 have been performed that do include embodied emissions. First, NETL performed detailed analyses of SMR systems, finding 16.4 kg CO_2eq./kg H_2 for the case without CCS and 8.9 kg CO_2eq./kg H_2 for the case with CCS.[43] Kanz et al. (2021) found an average CI for solar-PV-derived H_2 of 3.6 kg CO_2/kg H_2, with a 95% CI on the empirical data of 1.1 – 6.4 kg CO_2eq./kg H_2 (Min-Max = 0.7 – 6.6).[44] Numerous other studies exist, but there is little consensus in the literature, with Kanz et al. noting that only 14 of 33 studies could be harmonized due to lack of open data, and stated that "Due to the lack of transparency of most LCAs included in this review, full identification of the sources of discrepancies (methods applied, assumed production conditions) is not possible."[44] Despite this uncertainty, the values estimated here for geologic H_2 lower than those of green and blue H_2 for most near-term modeling cases (that include embodied emissions).

Importantly, the GWP of H_2 is a matter of some recent debate, with 100-year GWPs in recent studies varying by a factor of 3 or so from the lowest to highest estimates. In this study, it does not appear that shifting from our baseline GWP_{100} of 5 to a high estimate of 11 results in major changes to the GHG intensity (see Figure 4). Shifting to a GWP_{20} instead of the OPGEE default of GWP_{100} would have a larger impact, but in that case other sources such as natural gas would also have higher GHG intensity.

A key factor in low-CI production is the source of energy to power and heat for compression and gas processing. These results suggest that H_2 could be a low carbon source of energy if the gas is produced responsibly, and the system is powered by low carbon energy sources, either by self-produced clean H_2, or by purchased certified green power (e.g., "Electric – RECS" case above).

The baseline case has a production-weighted average CI for extraction and processing of ~3 gCO_2 eq./MJ, or ~20-33% the production CI of conventional natural gas sources. Additionally, the end-product H_2 has no combustion CI, compared to ~50 gCO_2eq./MJ for natural gas. Thus, the overall life cycle CI for geologic hydrogen (including transport and end-use of the gas -- though not modeled explicitly here) is likely to exhibit a 90-95% reduction compared to conventional gas. Additional work to verify these reductions should be performed when commercial projects are developed and more detailed process engineering data are available for analysis.

Acknowledgements

This work was funded by Smart Gas Sciences LLC as an independent consulting project separately from Dr. Brandt's position at Stanford University.

Works Cited

1. Zgonnik, V. The occurrence and geoscience of natural hydrogen: A comprehensive review. *Earth-Science Reviews*. 2020. https://doi.org/10.1016/j.earscirev.2020.103140
2. Arrouvel, C. and Prinzhofer, A. Genesis of natural hydrogen: New insights from thermodynamic simulations. *International Journal of Hydrogen Energy*. 46 (2021) 18780e18794. DOI https://doi.org/10.1016/j.ijhydene.2021.03.057
3. Hand, E. Hidden Hydrogen: Does Earth hold vast stores of a renewable, carbon-free fuel? Science 2023 379(6633). DOI: 10.1126/science.adh1477
4. Worman, S.L.; Pratson, L.F. et al. Abiotic hydrogen (H_2) sources and sinks near the mid-ocean ridge (MOR) with implications for the subseafloor biosphere. Proceedings of the National Academy of Sciences (2020). 117, 24. DOI: 10.1073/pnas.2002619117
5. Proskurowski, G. Lilley, M.D. et al. Low temperature volatile production at the Lost City Hydrothermal Field, evidence from a hydrogen stable isotope geothermometer. *Chemical Geology* (2006) 331-343. DOI: https://doi.org/10.1016/j.chemgeo.2005.11.005
6. Guelard, J., V. Beaumont, et al. (2017), Natural H_2 in Kansas: Deep or shallow origin?, *Geochem. Geophys. Geosyst*., 18, 1841–1865, doi:10.1002/ 2016GC006544.
7. Sherwood-Lollar, B., Voglesonger, K. et al. Hydrogeologic controls on episodic H_2 release from precarmbrian fractured rocks – Energy for deep subsurface life on Earth and Mars. Astrobiology 2007, 6. DOI: 10.1089/ast.2006.0096
8. Abranjano, T.A.; Sturchio, N.C. et al. Methane-hydrogen gas seeps, Cambalaes ophiolite, Phillipines: Deep or shallow origin? Chemical Geology, 71, (1988) 211-222.
9. Boreham, C.J.; Edwards, D.S., et al. Hydrogen in Australian natural gas: Occurences, sources, and resources. The APPEA Journal. 2021, 61, 163-191. DOI: https://doi.org/10.1071/AJ20044
10. Donze, F.-V.; Truche, L. et al. Migration of natural hydrogen from deep-seated sources in the Sao Francisco basin, Brazil. Geosciences 2020, 10, 346. DOI: 10.3390/geosciences10090346
11. Leong, J.A. et al. H_2 and CH_4 outgassing rates in the Samail ophiolite, Oman: Implications for low-temperature, continental serpentinization rates, Geochimica et Cosmochimica Acta, 347 (2023) DOI: 10.1016/j.gca.2023.02.008.
12. Vacquand, C.; Deville, E. et al. Reduced gas seepages in ophiolitic complexes: Evidences for multiple origins of the H_2-CH_4-N_2 gas mixtures. Geochimica et Cosmochimica Acta 223 (2018) 437–461. DOI: 10.1016/j.gca.2017.12.018
13. Prinzhofer, A. Cisse, C.S.T. et al. 2018. Discovery of a large accumulation of natural hydrogen in Bourakebougou (Mali). *International Journal of Hydrogen Energy* 43 (2018) 19315e19326. DOI: 10.1016/j.ijhydene.2018.08.193
14. Bergerson, JA, Brandt, AR, Cresko, J, et al. Life cycle assessment of emerging technologies: Evaluation techniques at different stages of market and technical maturity. *Journal of Industrial Ecol*ogy 2020; 24: 11– 25. https://doi.org/10.1111/jiec.12954
15. El-Houjeiri, H. M. A.R. Brandt, J.E. Duffy (2013). Open-source LCA tool for estimating greenhouse gas emissions from crude oil production using field characteristics. Environmental Science & Technology 47(11): 5998-6006. DOI: 10.1021/es304570m
16. M.S. Masnadi, G. Benini , A. Milivinti , J.E. Anderson , T.J. Wallington , R. De Kleine , V. Dotti , P. Jochem , H. El-Houjeiri , A.R. Brandt. Carbon implications of global marginal oils: market- derived displacement effects of short-term demand shocks. Nature. DOI: 10.1038/s41586-021- 03932-2
17. S. Sleep, Z. Dadashi, Y. Chen, A.R. Brandt, H.L. MacLean, J.A. Bergerson. Improving ro- bustness of LCA results through stakeholder engagement: A case study of emerging oil sands technologies. Journal of Cleaner Production. DOI: 10.1016/j.jclepro.2020.125277

18. Nie, Y., S. Zhang, R.E. Liu, D.J. Roda-Stuart, A.P. Ravikumar, A. Bradley, M.S. Masnadi, A.R. Brandt, J. Bergerson, X. Bi. Greenhouse-gas Emissions of Canadian Liquefied Natural Gas for Power Generation and District Heating in China: Three Independent Life Cycle Assessments. Journal of Cleaner Production DOI: 10.1016/j.jclepro.2020.120701
19. Masnadi, M.S., H.M. El-Houjeiri, D. Schunack, Y. Li, J.G. Englander, A. Badahdah, J.E. Anderson, T.J. Wallington, J.A. Bergerson, D. Gordon, S. Przesmitzki, I.L. Azevedo, G. Cooney, J.E. Duffy, G.A. Keoleian, C. McGlade, D.N. Meehan, T.J. Skone, F. You, M.Q. Wang, A.R. Brandt. Global carbon intensity of crude oil production. Science. DOI: 10.1126/science.aar6859
20. Masnadi, M.S., A.R. Brandt. Climate impacts of oil extraction increase significantly with oilfield age. Nature Climate Change. DOI: 10.1038/nclimate3347
21. Cooney, G., M. Jamieson, J. Marriott, J. Bergerson, A.R. Brandt, T.J. Skone. Updating the US life cycle GHG petroleum baseline to 2014 with projections to 2014 using open-source engineering-based models. Environmental Science & Technology DOI: 10.1021/acs.est.6b02819
22. Brandt, A.R., Masnadi, M.S., et al. Oil Production Greenhouse Gas Emissions Estimator OPGEE v3.0b: User guide & Technical documentation. 2022. Stanford University working paper. April 2022. From: https://eao.stanford.edu/
23. U.S. Department of Energy Clean Hydrogen Production Standard (CHPS) Draft Guidance. US Department of Energy, https://www.hydrogen.energy.gov/pdfs/clean-hydrogen-production-standard.pdf
24. Lemmon, E.W., Huber, M.L., McLinden, M.O. (2013) NIST Standard Reference Database 23: Reference Fluid Thermodynamic and Transport Properties-REFPROP, Version 9.1., National Institute of Standards and Technology, Standard Reference Data Program, Gaithersburg, 2013.
25. NIST 2022. Hydrogen properties: Henry's Law Constants. NIST Standard Reference Database 69: *NIST Chemistry WebBook.* https://doi.org/10.18434/T4D303
26. I.B. Ocko and S.P. Hamburg (2022). Climate consequences of hydrogen emissions *Atmos. Chem. Phys*., 22, 9349–9368, 2022. https://doi.org/10.5194/acp-22-9349-2022
27. R.G. Derwent, D.S. Stevenson, S.R. Utembe, M.E. Jenkin, A.H. Khan, D.E.. Shallcross (2020). Global modelling studies of hydrogen and its isotopomers using STOCHEM-CRI: Likely radiative forcing consequences of a future hydrogen economy. *International Journal of Hydrogen Energy*, https://doi.org/10.1016/j.ijhydene.2020.01.125.
28. Derwent, R.G., Simmonds P. Global environmental impacts of the hydrogen economy. Int J. Nuclear Hydrogen Production and Application. DOI:10.1504/IJNHPA.2006.009869
29. R.G. Derwent (2018). Hydrogen for heating: Atmospheric impacts. A literature review. BEIS Research Paper Number 2018: no. 21. UK Department for Business, Energy, and Industrial Strategy.
30. Warwick, N., Griffiths, P., Keeble, J., Archibald, A., Pyle, J., and Shine, K. (2022). Atmospheric implications of increased Hydrogen use, Department for Business, Energy and Industrial Strategy, 75 pp., https://www.gov.uk/government/publications/ atmospheric-implications-of-increased-hydrogen-use.
31. Warwick, N.J.; Bekki, S.; et al. Impact of a hydrogen economy on the stratosphere and troposphere studied in a 2-D model. Geophysical Research Letters. 31, 2004. DOI: 10.1029/2003GL019224
32. Huang, P.H. Humidity standard of compressed hydrogen for fuel cell technology. ECS Transactions: 12(1) 479-484 (2008). DOI: 10.1149/1.2921574
33. K.D. Luks, P.O.. Fitzgibbon, and J.T. Banchero. Correlation of the Equilibrium Moisture Content of Air and of Mixtures of Oxygen and Nitrogen for Temperatures in the Range of 230 to 600 K at Pressures up to 200 Atm. *Industrial & Engineering Chemistry Process Design and Development*, 1976, 15(2), 326 – 332, DOI: 10.1021/i260058a019.
34. Argonne National Laboratory. Hydrogen Delivery Scenario Analysis Model (HDSAM). Accessed March 5th 2023. https://hdsam.es.anl.gov/index.php?content=hdsam
35. Coker, A. Kayode. (2010). *Ludwig's Applied Process Design for Chemical and Petrochemical Plants, Volume 2 (4th Edition). Chapter 11: Petroleum, Complex-Mixture Fractionation, Gas Processing, Dehydration.*
36. Benson, H. and Celin, A. Recovering hydrogen – and profits – from hydrogen-rich offgas. CEP magazine. January 2018. pp. 55-59.
37. Du,Z.;Liu,C.; et al. A Review of Hydrogen Purification Technologies for Fuel Cell Vehicles. *Catalysts* 2021, 11, 393. https:// doi.org/10.3390/catal11030393
38. Dolan, S.L.; Heath. G.A.. Life Cycle Greenhouse Gas Emissions of Utility-Scale Wind Power: Systematic Review and Harmonization. *Journal of Industrial Ecology*. 2012. DOI: 10.1111/j.1530-9290.2012.00464.x

39. Hsu, D.; O'Donoughue, P.; Fthenakis, V.; Heath, G; Kim, H.; Sawyer, P.; Choi, J.; Turney, D. (2012). Life Cycle Greenhouse Gas Emissions of Crystalline Silicon Photovoltaic Electricity Generation: Systematic Review and Harmonization. Journal of Industrial Ecology (16:S1); pp. S122-S135. DOI: 10.1111/j.1530-9290.2011.00439.x
40. Omara, M. Zimmerman, N. et al. Methane Emissions from Natural Gas Production Sites in the United States: Data Synthesis and National Estimate. *Environmental Science & Technology*. 2018 52 (21), 12915-12925. DOI: 10.1021/acs.est.8b03535
41. Rutherford, J.S., Sherwin, E.D., *et al.* Closing the methane gap in US oil and natural gas production emissions inventories. *Nature Communications* 12, 4715 (2021). DOI: 10.1038/s41467-021-25017-4
42. Elgowainy, A. 2022. GREET model for Hydrogen Life Cycle GHG emissions. Argonne National Laboratory. Presentation at H2IQ webinar, June 15th, 2022.
43. Lewis, E. et al. Comparison of commercial, state-of-the-art, fossil-based hydrogen production technologies. National Energy Technology Laboratory. April 12th, 2022. DOE/NETL-2022/3241.
44. Kanz, O. et al. Review and Harmonization of the Life-Cycle Global Warming Impact of PV-Powered Hydrogen Production by Electrolysis. Frontiers in Electronics. doi: 10.3389/felec.2021.711103.

Supporting information for "Greenhouse gas intensity of geologic hydrogen produced from subsurface deposits"

Adam R. Brandt
Department of Energy Science & Engineering
Stanford University
abrandt@stanford.edu
+1-650-724-8251

SI.1: Methods for average North America gas wells

In order to model geologic H_2 fields, we make a basic assumption, for the baseline case at least, that the geologic H_2 fields will look similar to North America gas wells in aggregate. We also explore sensitivity cases in which the gas may be, for example, more shallow or deeper than average US gas.

Data for North America gas wells is derived from Enverus, a commercial data provider that aggregates public data from states and provinces. The Enverus PRISM platform is used to access data. The following search filters are used within Enverus PRISM:

- The geographic window includes all of North America. As Enverus does not include data on Mexico, this dataset includes USA and Canada.
- We limit the search to wells that have been classified by Enverus as gas wells. This is done using the filter string ENV Well Type = "GAS".
- The resulting dataset includes 1,007,302 wells, as accessed on Feb 15th, 2023.
- Data on aggregate productivity for gas and water production by well vintage (e.g., well completion year) were exported as well as the underlying well property data.

SI.1.1: Estimated ultimate recovery (EUR) per well

To generate a figure for estimated ultimate recovery (EUR), we first filter the dataset to remove failed wells. The dataset of wells was filtered to include only wells with cumulative production to date of greater than 10,000 mcf of gas. This eliminates failed wells that produce little gas, and removes data errors. It also eliminates wells that report no gas production, with a blank value in the cumulative production column (many of these appear to be exploratory wells).

Estimated ultimate recovery can be assessed in two ways: (1) by examining cumulative production for wells that have been producing for a significant amount of time, and (2) by using reported EUR in the Enverus datasets. Unfortunately, the reported EUR columns are not available in Enverus PRISM datasets, so we use method 1.

Taking all wells in the dataset, regardless of vintage, we get the following summary statistics given in Table S1 below.

Table S1: Cumulative production statistics from Enverus PRISM, using the column "CumGas_MCF" and dividing by 1e6 to obtain BCF.

Parameter	Value	Unit
Well count	685661	Wells
Mean	1.33	BCF/well
Median	0.36	BCF/well
5th perc.	0.02	BCF/well
25th perc.	0.10	BCF/well
50th perc.	0.36	BCF/well
75 th perc.	1.21	BCF/well
95 th perc.	5.02	BCF/well
99 th perc.	12.98	BCF/well

While this dataset includes numerous newer wells, those tend to be very productive hydraulically fractured wells that have higher per-well productivity than seen historically in conventional gas wells.

We therefore choose a baseline EUR that is equal to the mean in the dataset (1.33 BCF), while a low case we set to 0.33 BCF per well, and a high case to 2 BCF per well.

From these statistics, we generate the following rounded case values for EUR:

Baseline: 1.33 BCF

Low productivity: 0.33 BCF

High productivity: 2 BCF

SI.1.2: Well depth

To estimate well depth, we take the same underlying dataset described above, and generate summary statistics for true vertical depth of the well, the best measure of sub-surface depth (more accurate than measured well depth that includes deviation and horizontal sections).

The column "TVD_FT" is extracted from the dataset. Values of 0 and missing values (blanks) are filtered from the dataset. The resulting TVD data are presented below in

Parameter	Value	Unit
Well count	876,456	Wells
Mean	6,007	ft
Median	5,247	ft
5th perc.	1,509	ft

25th perc.	2,830	ft
50th perc.	5,247	ft
75 th perc.	8,432	ft
95 th perc.	12,981	ft
99 th perc.	15,922	ft

From these we generate the following rounded case values for depth at roughly the mean, 5th and 95th percentiles.

Baseline: 6,000 ft

Shallow: 1,500 ft

Deep: 12,000 ft

Note that the deep well is similar in depth to the well drilled in Nebraska by Natural Hydrogen Energy.

SI.1.3: Water production

Using the same filters as the EUR and cumulative production dataset above, we also extract data on cumulative water production for each well from the column "CumWater_BBL".

We eliminate the following wells from the dataset:

- Less than 10,000 mcf cumulative production, including wells with "blank" values in the cumulative production column. These are the same filters as above.
- Wells with "blank" values for water production. We leave wells in the dataset that report an actual 0 value for water production, as dry gas wells do exist that produce essentially no water. We do not know how many of these 0 values are actually 0 values or are simply not reported by the agency that generates the underlying data.

The following summary statistics are generated for WOR for the producing wells:

Parameter	**Value**	**Unit**
Well count	685,664	Wells
Mean	65.683	bbl water/mmscf
Median	0.000	bbl water/mmscf
5th perc.	0.000	bbl water/mmscf
25th perc.	0.000	bbl water/mmscf
50th perc.	0.000	bbl water/mmscf
75 th perc.	9.347	bbl water/mmscf
95 th perc.	161.062	bbl water/mmscf
99 th perc.	912.872	bbl water/mmscf

As can be seen, these data are highly skewed, with many 0 values. For simplicity and to assume a case where there is some water production, we choose the following baseline value: 1 bbl water per mmscf. We do not explore sensitivity cases because water handling is generally a very small contributor to CI.

SI.1.3: Production decline rate

Production decline rate is taken from the same Enverus datasets as above. A total of 160,229 wells in the dataset have >360 months of production data. Taking this group of wells and aligning all wells to start at month 1, cumulative production is generated as a function of month for months 1-360. This cumulative series is then differenced to get monthly production. We then group into years Y1-Y30. We excise the potentially sensitive or proprietary production volumes, but present yearly production changes for this dataset changes as follows:

Year	Start month	End month	Percent of last year	YoY fractional decline
Y1	1	12	NA	NA
Y2	13	24	0.71905352	0.28
Y3	25	36	0.81101724	0.19
Y4	37	48	0.84642628	0.15
Y5	49	60	0.87390935	0.13
Y6	61	72	0.89279085	0.11
Y7	73	84	0.90316241	0.10
Y8	85	96	0.91396722	0.09
Y9	97	108	0.91807407	0.08
Y10	109	120	0.93018785	0.07
Y11	121	132	0.93636355	0.06
Y12	133	144	0.93529922	0.06
Y13	145	156	0.94367216	0.06
Y14	157	168	0.95041268	0.05
Y15	169	180	0.96127881	0.04
Y16	181	192	0.9696061	0.03
Y17	193	204	0.96450071	0.04
Y18	205	216	0.97569056	0.02
Y19	217	228	0.97585275	0.02
Y20	229	240	0.97592745	0.02
Y21	241	252	0.96370657	0.04
Y22	253	264	0.96716407	0.03
Y23	265	276	0.97248525	0.03
Y24	277	288	0.96994038	0.03

Y25	289	300	0.98301154	0.02
Y26	301	312	0.95842596	0.04
Y27	313	324	0.97906852	0.02
Y28	325	336	0.95737569	0.04
Y29	337	348	0.96898727	0.03
Y30	349	360	0.9716936	0.03

These production decline rates are used as our default production decline rates.

SI.2: Comparison of compression energy estimates for streams containing H_2

Because the OPGEE model was not designed to model significant amounts of H_2, we wanted to compare our compression energy calculations to established hydrogen compression models. We compared OPGEE results to the "Hydrogen Delivery Scenario Analysis Model, HDSAM version 3.1 (Argonne National Laboratory).

HDSAM sheet "H_2 Compressor" was used as the comparison point. We then adjusted a version of OPGEE to model the same system outlined on that sheet:

- Composition: 100% H_2
- Inlet pressure 20 atm (converted to 294 psi for OPGEE input)
- Outlet pressure 68 atm (converted to 999 psi for OPGEE input)
- Inlet temperature 25 °C (converted to 77 °F for OPGEE input)
- 2 stages of compression
- Flow rate of H_2 to compressor: 13.376 tonne H_2 /d

After modifying OPGEE appropriately to allow this configuration, the following results were found:

- Adiabatic work of compression: 264 kW
- Required brake horsepower: 352 kW
- Electricity consumed by motor: 368 kW

The HDSAM model, on the other hand, finds:

- Theoretical power requirement: 262 kW
- Actual shaft power requirement: 298 kW
- Motor rating per compressor: 347 kW

Our conversion from theoretical work of compression to brake horsepower uses an efficiency of 75%, while HDSAM assumes an isentropic efficiency of 88%. However, the HDSAM model assumes a motor efficiency of 94% and motor oversizing of 110% of required power.

Overall, the OPGEE compressor model lines up well, though not exactly, with the HDSAM model.